Collisions of Spherical Galaxies

Junichiro Makino
Institute for Advanced Study
Princeton, NJ 08540 USA
Department of Earth Sciences and Astronomy
College of Arts and Sciences, University of Tokyo
3-8-1 Komaba, Megro-ku, Tokyo 153, Japan

Piet Hut
Institute for Advanced Study
Princeton, NJ 08540 USA

Abstract

We have performed a systematic survey of collisions of two identical spherical galaxies. In doing so, we determined a criterion for the occurrence of merging between two galaxies, expressed as a merging line in terms of the relative velocity and impact parameter at infinite relative distance. We have also determined the relation of the mass loss and loss of internal and orbital energy of galaxies to the collision parameters for both the merging and the non-merging case. For the initial galaxy model, we have used several King models with different values for the central potential as well as a Plummer model. In the non-merging case, the impulse approximation used in previous studies (Aguilar and White, 1985) turned out to be acceptable, although large difference were found for initial conditions close to the merging line. The mass loss depends strongly on the initial configuration of the galaxy, especially for collisions with a large impact parameter. For both internal and orbital energy the amount of change shows a much weaker dependence on the initial configuration. Consequently, the merging line also depends only weakly on the type of the initial galaxy. In the merging case, in all hyperbolic and parabolic encounters we observed slowly rotating significantly prolate galaxies. In encounters from bound orbits, end products are triaxial or oblate, depending on the initial angular momentum and periastron distance. The detailed results of our study have many applications. An example would be to use the present results, converted to cross sections and reaction rates, to determine the macroscopic evolution of a whole cluster of galaxies.

Introduction

Galaxy-galaxy encounters have been sufficiently frequent in the history of the universe and galaxy-galaxy scattering is sufficiently inelastic that it is possible that a substantial portion of the "normal" galaxies that we observe today have undergone mergers or less drastic encounters. Indeed, many observed systems are classified as interacting or merging galaxies on the basis of definite structural features such as tidal bridges and tails extending from disk galaxies, and faint shells of starlight surrounding elliptical galaxies.

Some of the more spectacular examples observed can be impressively reproduced by careful analysis of particular collision geometries. Our present understanding of galaxy-galaxy collisions, and the merging processes which they can cause, would have been impossible to obtain from either observations or computations alone. Computations are essential to provide a plausible history for interpreting observations, which are necessarily only "snapshots" given the brevity of human life from a cosmic perspective.

Toomre and Toomre (1972) first showed that a number of galaxies with very irregular shape can be explained as the remnant of the collision of two galaxies. They modeled a galaxy by a heavy point mass and mass-less particles which orbit around that point mass. When two such "galaxies" collide, the spatial structure showed strikingly good agreement with the observed irregular galaxies. Barnes (1988) performed a self-consistent calculation of mergers which included a realistic, self-gravitating heavy halo of dark matter. He concluded that the merger remnant, formed by the collision of two spiral galaxies, shows a striking resemblance with elliptical galaxies (see Figure 1).

The effect of collisions on the evolution of the galaxies is, however, still largely unknown. For example, no one has yet determined a quantitative merging criterion, except for the simplest case of head-on collisions of two identical spherical galaxies (van Albada and van Gorkom 1977). The most systematic research concerning the dependency on collision parameters of the distortion of colliding galaxies was performed by Aguilar and White (1985, 1986), who employed the impulse approximation to evaluate the effect of collisions for a wide range of initial galaxies and collision parameters. Their results, however,

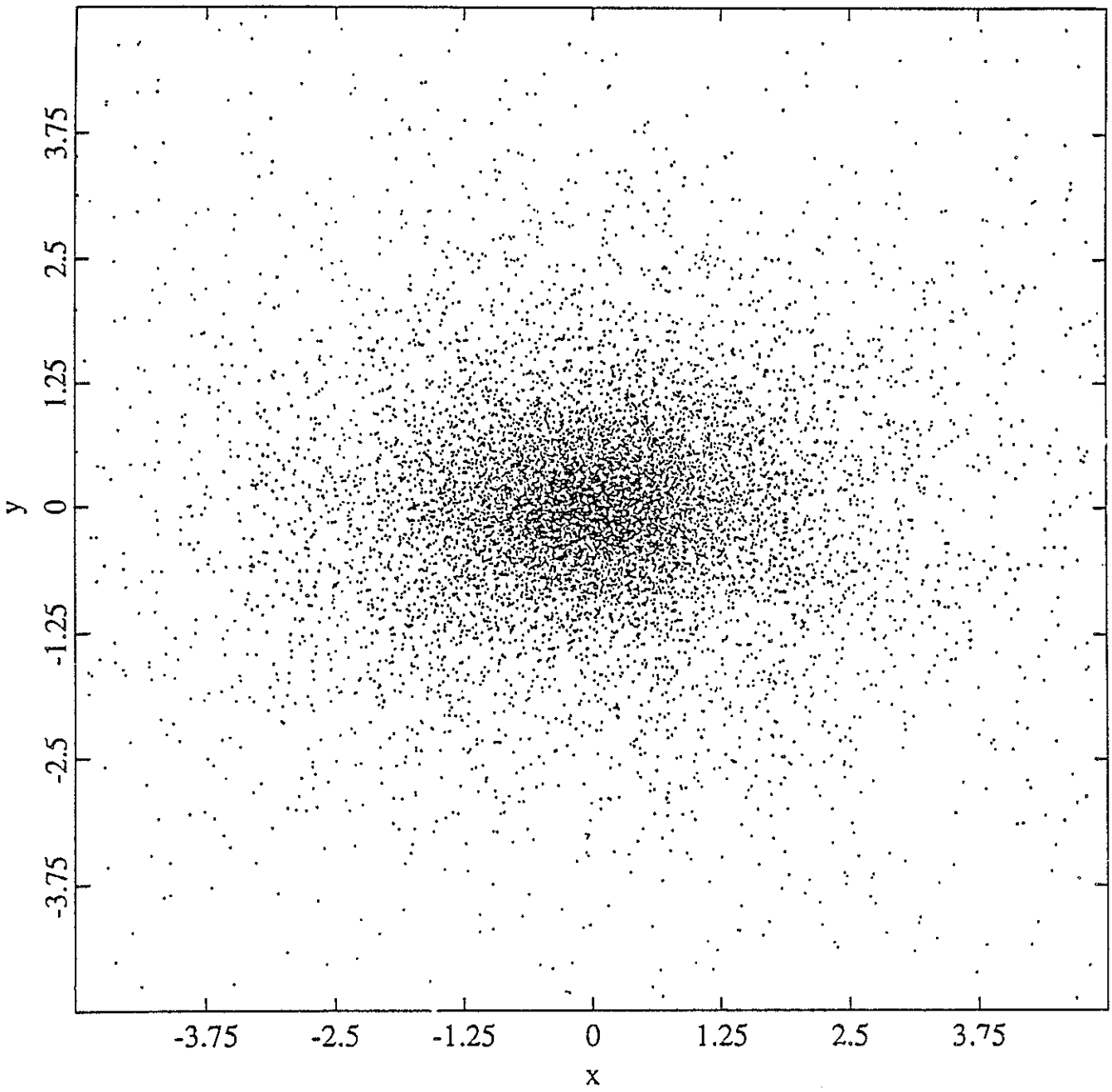

Figure 1: A merger remnant, formed after a collision between two galaxies.

have two limitations. Firstly, the impulse approximation is not reliable when applied to the slow collisions in which the relative velocity of the two galaxies is not much larger than the r.m.s. velocity of stars within the galaxies, because the impulse approximation is based on the assumption that the root mean square (r.m.s.) velocity of stars in the galaxy is much smaller than the relative velocity of colliding galaxies. Secondly, the impulse approximation gives us no information about the structure of the galaxies after collision. In Aguilar and White (1986), they used an N-body method to study the shape of galaxies after the collision. In their calculation, however, one of the two galaxies was represented by a fixed potential well. Therefore the applicability of their results is limited to "weak" collisions, where the change in the structure of the galaxies during the collision can be ignored. Moreover, their method cannot deal with mergers.

A self-consistent N-body calculation is clearly desirable, because it gives much more detailed information than more approximate methods. The N-body method is, however, more computationally expensive than other methods by several orders of magnitude. In previous works, many different methods have been developed to reduce the cost of N-body calculations (Miller and

Smith 1978, van Albada and van Gorkom 1977, Villumsen 1982, White 1983). All methods rely on some form of expansion to represent the potential fields. Thus they inevitably have some limitation in the geometry and/or spatial resolution. Moreover, even these expansion methods were expensive when they were first developed and no one has yet tried to run more than a few tens of simulations. Thus, published results are essentially the description of individual collision experiments, and very little discussion has appeared concerning the quantitative dependency of the results on the collision parameters.

In this paper, we describe the results of more than two hundred collision experiments performed by a fully self-consistent direct N-body method. All collisions are for galaxies with the same total mass and total energy. Each initial galaxy is spherical and not rotating. This is the simplest example of galactic encounters. In the next section we describe the numerical method and initial conditions. We used 2048 particles per galaxy for all experiments. We then describe the results. It turned out that the impulse approximation(Aguilar and White 1985) is quite good. We also give the loss of orbital energy, and a quantitative merging criterion. For mergers, we discuss their shape and its evolution. In hyperbolic and parabolic encounters the merger remnant is significantly prolate and slowly rotating. In encounters from bound orbits, the merger is triaxial to oblate, depending on the initial angular momentum and periastron distance of the initial orbit. At present, the number of particles per galaxy is still too small to allow a detailed analysis of the three-dimensional structure of the galaxies after collision, though it is large enough to determine the change in global parameters such as the total mass and the total energy.

Description of the Experiments

Numerical Method

In our experiment, the orbit of each star in our system is integrated directly by applying the equation of motion:

$$\frac{d^2 \mathbf{r}_i}{dt^2} = \sum_{j \neq i} \frac{G m_j (\mathbf{r}_i - \mathbf{r}_j)}{[(\mathbf{r}_i - \mathbf{r}_j)^2 + \varepsilon^2]^{3/2}} \qquad (1)$$

where $\mathbf{r}_i$ is the position of the ith particle, m_i is the mass of the ith particle, and G is the gravitational constant. The constant ε is the potential-softening parameter, which is introduced in order to avoid the singularity in the potential that otherwise causes numerical difficulties.

We calculate the acceleration on each particle directly by using equation (1). All particles share the same timestep. Thus the total computational cost is $O(N^2)$, where N is the number of particles in the system. As the time integrator we used the zero-order predictor and first-order corrector method, which is equivalent to the time-centered leap-frog scheme but has the advantage that the truncation error can be estimated in a simple way.

A number of efforts have been made to reduce the computational cost of the N-body integration. These efforts can be classified into two different groups. One approach is to try to reduce the number of force calculations by introducing more sophisticated integration schemes (for recent a review, see Aarseth 1985). The other approach is to reduce the cost-per-force calculation. The latter includes particle-mesh schemes, particle-particle particle-mesh schemes, spherical harmonics methods, and the tree algorithms (Appel 1985, Porter 1985, Jernigan 1985, Barnes and Hut 1986, Press 1986, Greengard and Rokhlin 1987). However, all these sophisticated methods turned out to be either inappropriate or inefficient. An Aarseth-type scheme does not improve the efficiency unless the size of the softening parameter ε is much smaller than the average interparticle distance. The expansion schemes are not appropriate because of their limited spatial resolution. Finally, the tree algorithm does not provide much improvement over the direct summation for a number of particles $N \approx 4000$.

The total number of particles used is 4096 for most of our calculations. For all experiments described in this paper, we have used a new ETA10 supercomputer at the John von Neumann National Supercomputer Center. One step of integration takes ~1.5 second on a ETA10-E running at the 10.5 ns clock cycle, using 32-bit arithmetic and utilizing one processor. The time span of our simulation is about 20 initial crossing times and the number of time steps is about 3000. Thus one experiment took ~75 minutes. The total energy is conserved to 0.1 ~1%. In the appendix we show the results of timing benchmarks for several supercomputers.

The Experiments

As the initial galaxy, we adopted four different spherical models: three King models with different values for the central potential (3, 5 and 7) and a Plummer model. All these models have an isotropic velocity distribution. As suggested by

Aguilar and White (1985), the difference in the velocity distribution is less important than the difference in the density distribution. For all calculations, initial galaxies are modeled by 2048 equal-mass particles. Thus the total number of particles is 4096.

We use standard units (Heggie and Mathieu 1986), *ie* G=1, M=1, E=-0.25, where G is the gravitational constant, M is the mass of one initial galaxy, E is the total energy of one initial galaxy. In this system of units the half mass radius of a Plummer model is $1/\sqrt{2}$. For King models it is about 0.75.

In this study we discuss the collisions of two galaxies which have the same initial structure. We performed four series of experiments for the four different types of galaxies. Figure 2 shows the collision parameters used in our experiments in terms of the relative velocity and the impact parameter at infinite relative distance. Filled circles indicate the basic series of experiments performed for all four initial galaxies. Open circles indicate additional calculations performed for the King model with W_c=3.

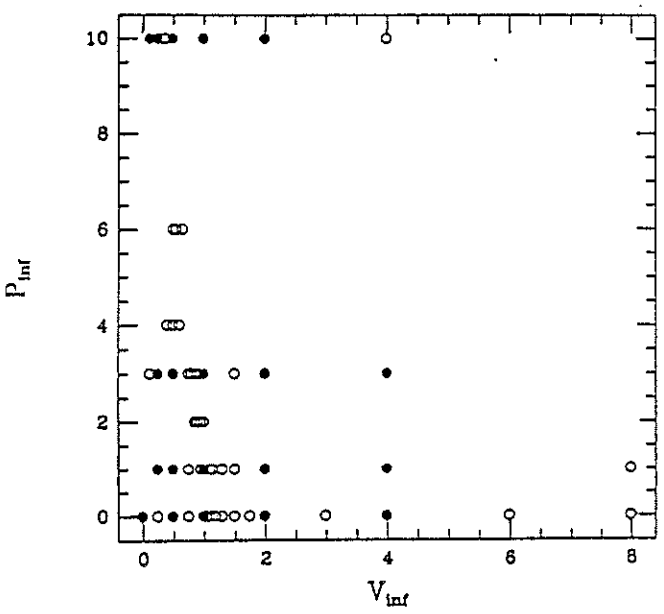

Figure 2: Distribution of the collision parameters used in this study, in terms of the relative velocity v_{inf} and the impact parameter P_{inf} at infinite relative distance. Filled circles indicate a standard set of collision parameters applied to all four initial galaxy models. Open circles indicate additional runs performed for the King model with non-dimensional central potential W_C=3. Most additional runs are performed to determine the merging criterion accurately.

Results

Merging criterion

Figure 3 shows the merging line, defined as the critical impact parameter below which merging occurs, as a function of the relative velocity at infinity. The solid line denotes the merging line for the King model with W_c=3 and the dashed line for the King model with W_c=7. Those two lines are remarkably close. For the Plummer model and King model with W_c=5, we did not determine the merging criterion to the accuracy we obtained for other models. The contour map for the loss of orbital energy indicates, however, that the Plummer model would show quite similar results with a King model with W_c=7, and the King model with W_c=5, naturally, would fall in between King models with W_c=3 and 7. Previous results were available only for head-on collisions. According to Roos and Norman, the critical velocity of merging obtained by van Albada and van Gorkom using their axially symmetric code is 3.2 σ at the maximum overlap, where σ is the internal velocity dispersion. If we assume that the shape of the potential does not change during the encounter, the relation between the relative velocity at infinity and that at maximum overlap is given by:

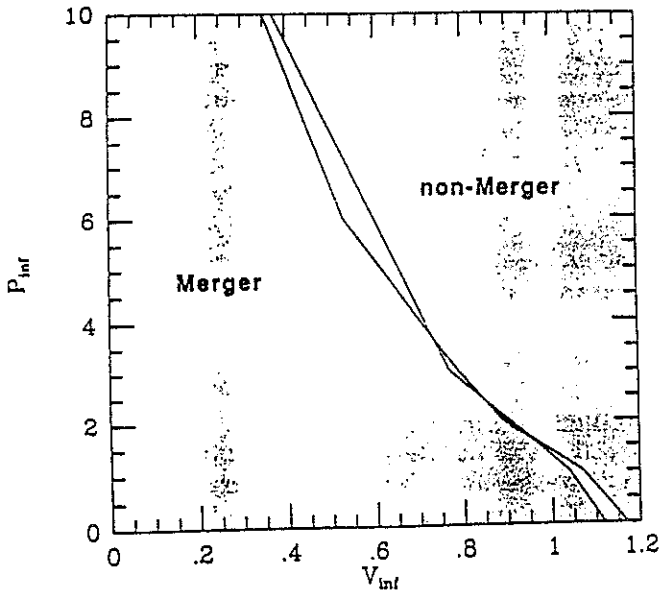

Figure 3: The critical impact parameter at infinity below which two galaxies will merge, as a function of the relative velocity at infinity. The solid line is for the King model with W_C=3 and the dotted line is for the King model with W_C=7. The difference between the two lines is marginally significant, and close to the experimental uncertainity.

$$\frac{1}{2}\mu v_{inf}^2 = \frac{1}{2}\mu v_{max}^2 + 4E_0$$

where μ is the reduced mass of the relative motion of two galaxies, v_{inf} is the relative velocity at the infinity, v_{max} is the relative velocity at the maximum overlap, and E_0 is the total energy of the initial galaxy. At the maximum overlap, the potential energy of the total system is four times as large as the potential energy of the initial galaxy. Thus, the additional potential energy is two times that of the initial galaxy and four times as large as the total energy of the initial galaxy. $\sigma=1/\sqrt{2}$ in our unit. Thus, $v_{max}=3.2\sigma$ is translated to $v_{inf}=1.06$, which shows good agreement with our result, in spite of the difference in the initial galaxy.

Mass Loss and Energy Loss

Figure 4 shows the contours for the mass loss, loss of internal energy, and loss of the orbital energy in the plane of v_{inf} and P_{inf} for the non-merging cases. In all figures, the change is larger for smaller velocity and smaller impact parameter. The energy loss, both for internal and orbital energy, is quite similar for all four models. The mass loss, however, is rather different for different initial galaxies. This tendency was also found by Aguilar and White (1985), who compared a King model with high central condensation [log $(r_t/r_c)=2.2$] and $r^{1/4}$ models with several different velocity structures.

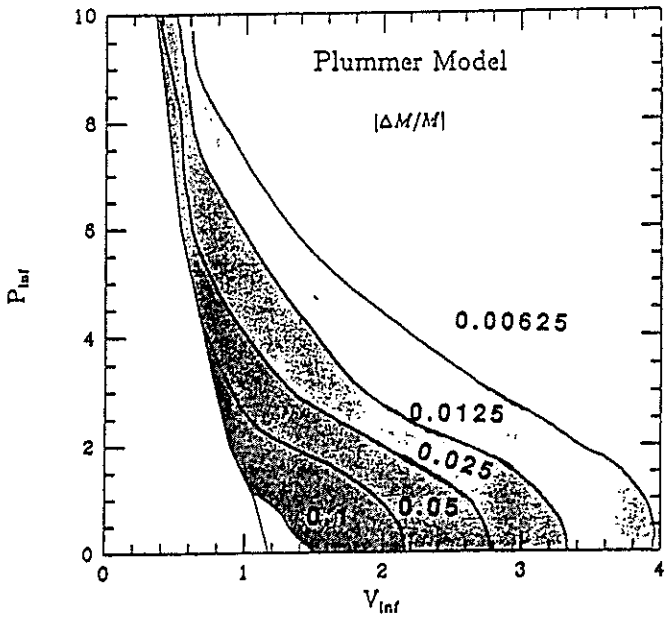

Above: Figure 4a.
At Right: Figure 4b,c,d.

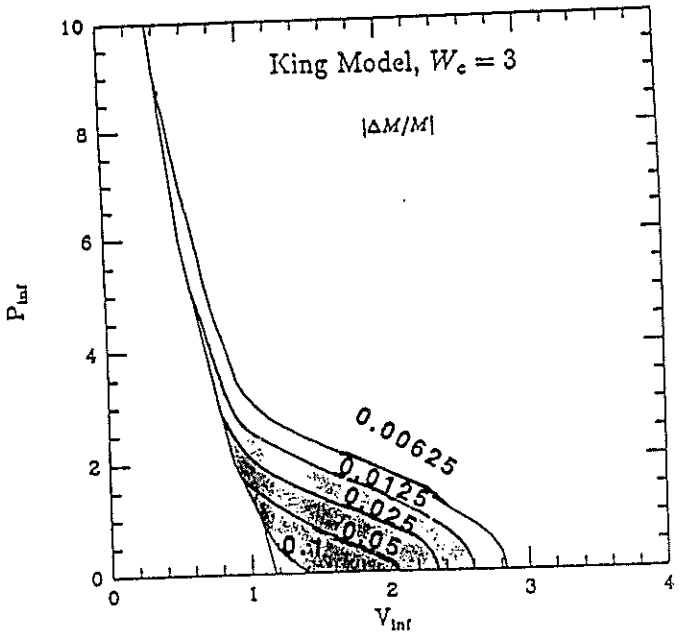

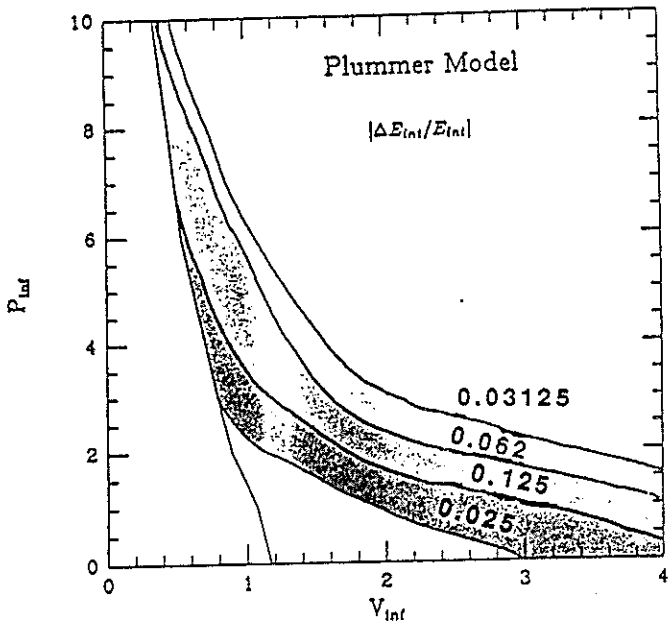

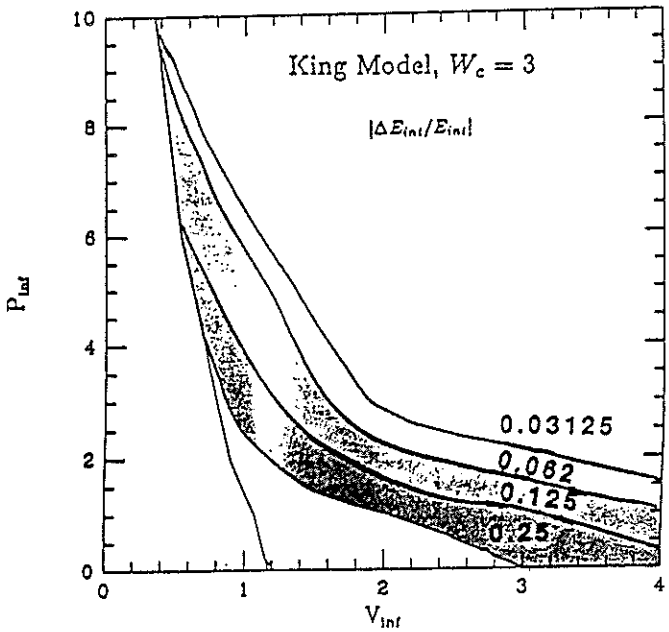

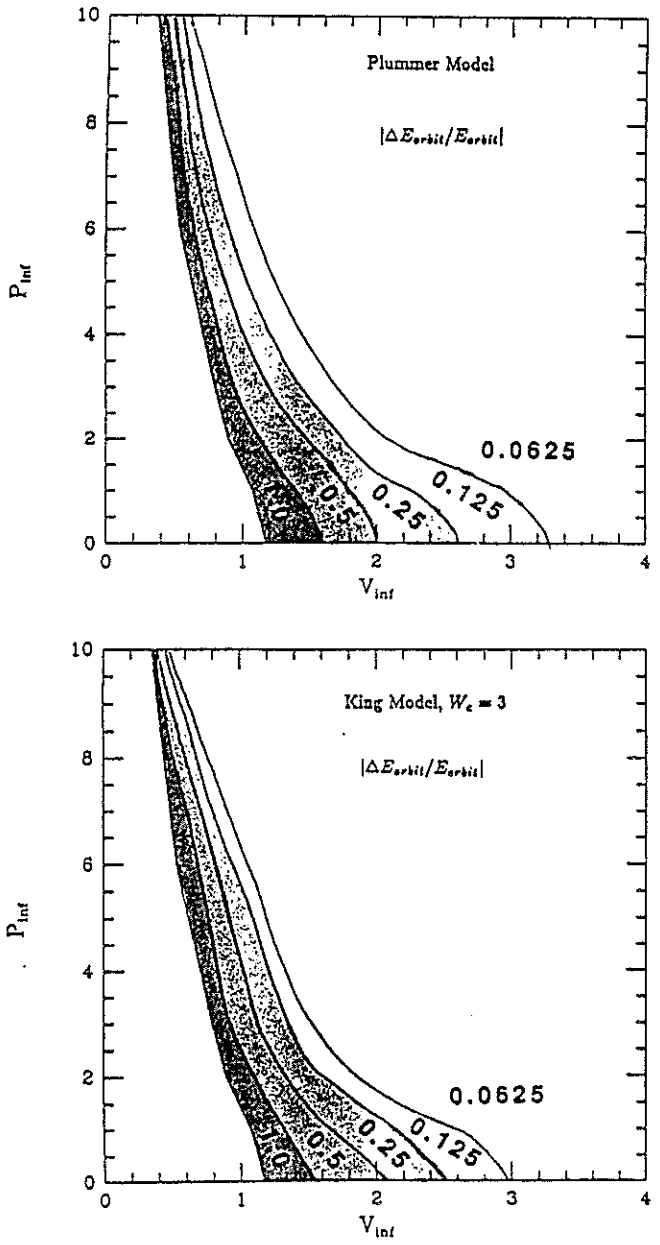

Figure 4 e and f: The contour map for the mass loss, the loss of the internal energy, and the loss of the orbital energy in the plane of the collision parameters v_{inf} and P_{inf}, for the King model with W_c=3 an d the Plummer model. The leftmost line indicates the merging line for the King model.

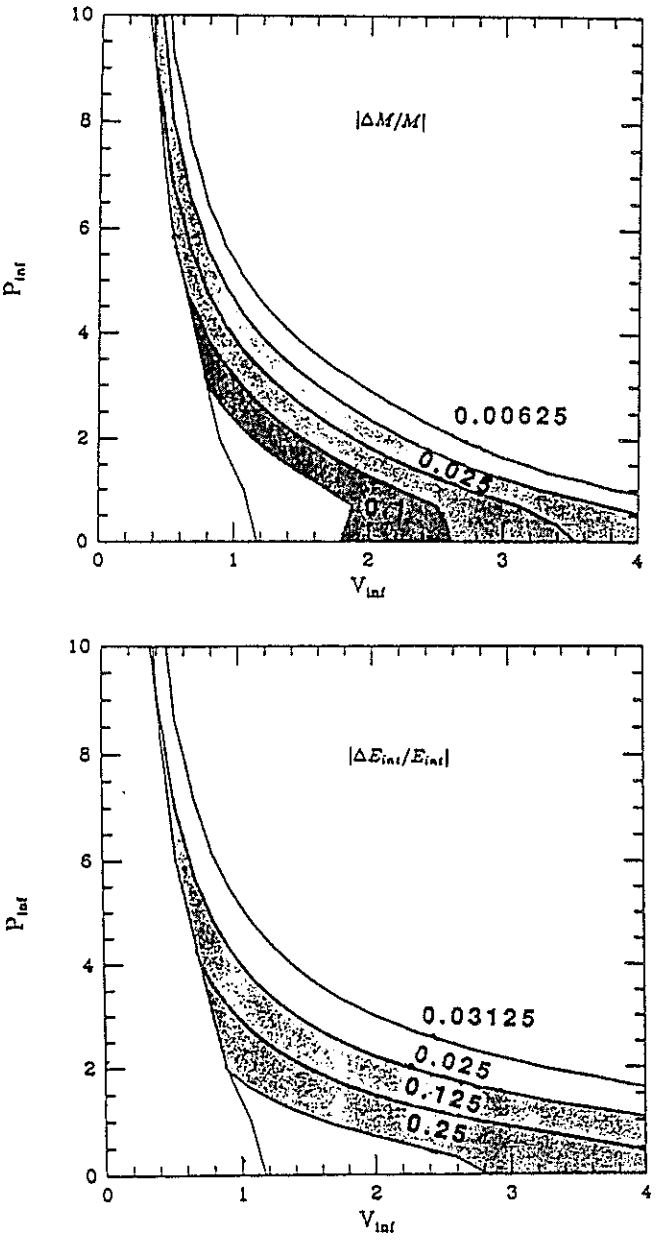

Figure 5: Same as figure 4 but obtained by the impulse approximation of Aguilar and White (1985) for a King model with very high central potential. (*cf.* their table 2)

Figure 5 shows the contours obtained using the fitting formula for the results of Aguilar and White (1985) for a King Model as given in their equations 9,10 and table 2. The agreement with our result for the Plummer model is quite good. It should be noted that the agreement with other previous studies is not very good. For example, van Albada and van Gorkom (1977) reported a mass loss of ~ 1% for the head on collision with v_{inf} =2.12. This is much smaller than what we observed, and the reason is not clear. It might be because their initial galaxy had a very sharp cutoff in the distribution function, which requires particles to gain more energy to reach the escape velocity.

Figure 6 shows the mass loss for merging cases. For a small impact parameter, the mass loss is larger for larger relative velocity. At first sight this looks strange, because the change of the energy of individual particles should be larger for smaller relative velocity. However, in the merg-

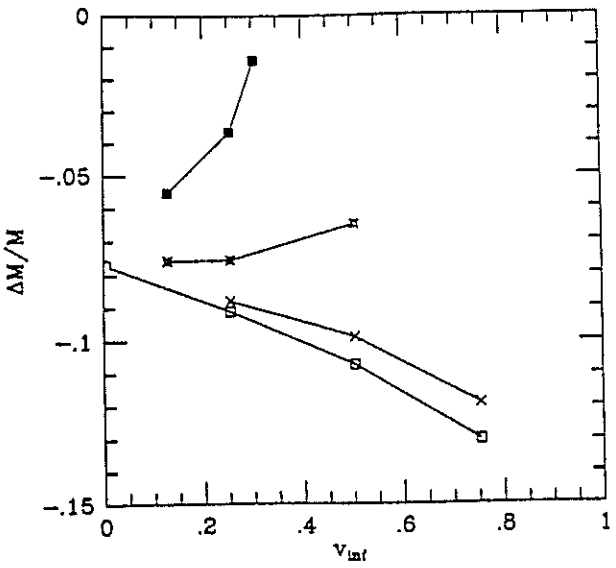

Figure 6: The amount of mass loss for the merging case as a function of v_{inf} for several values of P_{inf}. Open squares denote P_{inf}=0. Crosses, stars, and filled squares indicate P_{inf}=1, 3, 10, respectively.

ing case, whether a particle will escape from the system or not is determined by whether it is bound to the total system. With a larger initial velocity, particles are less bound to the total system because the absolute total energy is smaller. This explains why more particles escape for collisions with larger relative velocity. For larger impact parameter the mass loss quickly decreases, because an increase in the relative velocity results in an increase in the periastron distance. In the merging area, there has been no systematic study like that of Aguilar and White (1985), because the study of mergers requires full N-body calculations such as our present study. Moreover, most previous studies dealt with parabolic or elliptic initial conditions, which corresponds to binary galaxies. Villumsen (1982) showed several results for hyperbolic encounters. However, the criterion he used to define escapers seems to give significantly more escapers than our energy criterion and it is difficult to compare results. Simulations by White (1978, 1979) are consistent with our result.

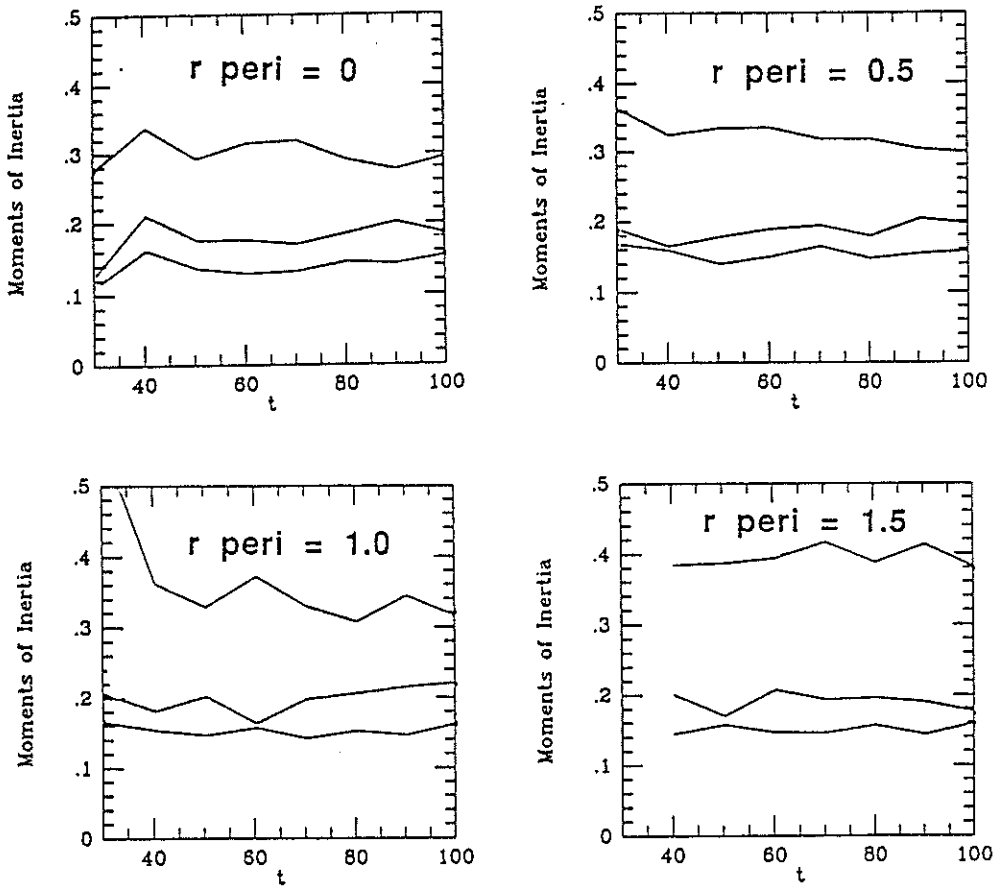

Figure 7: The evolution of the moments of inertia for the inner half-mass fraction bounded by an isodensity contour. Results are given for parabolic collisions with the periastron distance r_{peri}=0, 0.5, 1, 1.5.

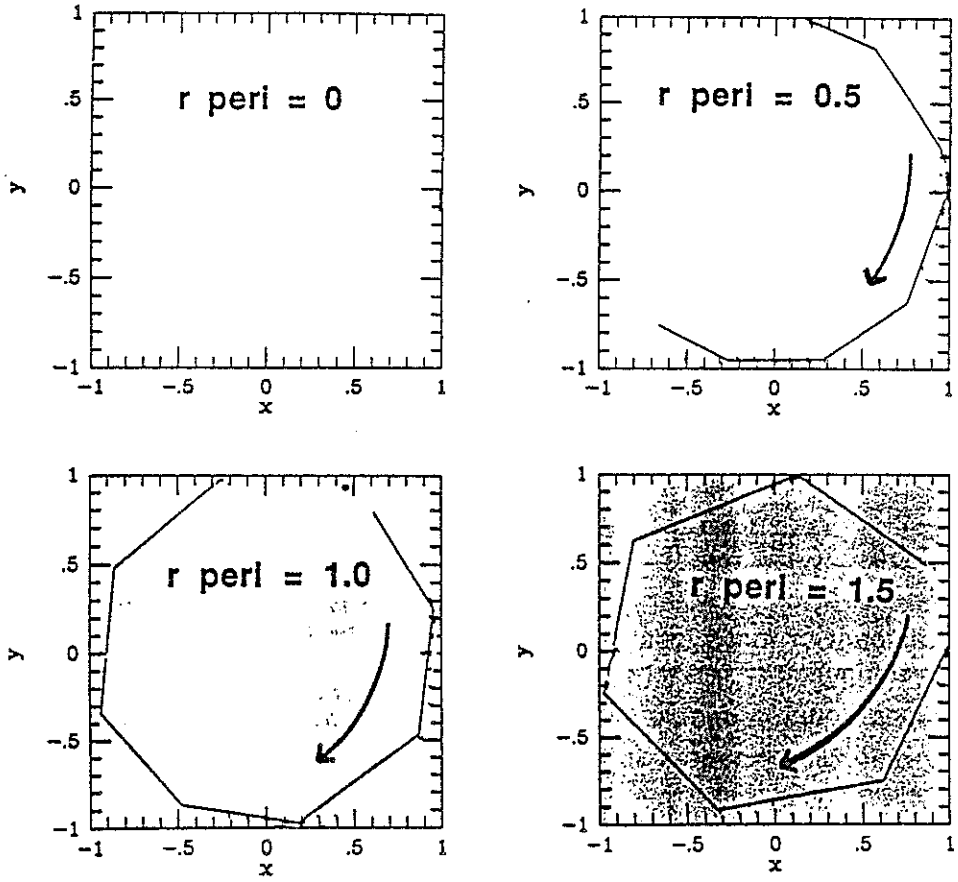

Figure 8: The trajectory of the normalized major axis vector in the x-y plane for parabolic collisions. Note that the major axis rotates more rapidly in the collisions with larger r_{peri}, for which the angular momentum of the total system is larger.

Structure of the Merger Remnant

It is extremely interesting to determine the detailed structure of the merger remnant and its dependency on the collision parameters from both a theoretical and an observational point of view. Intuitively, from head-on collisions we expect prolate merging remnant to emerge, elongated along the axis of the collision. For collisions with large angular momentum we expect oblate objects rotating along the axis of symmetry. In the intermediate case, we might expect triaxial objects to form which are slowly tumbling.

Figure 7 shows the components of the moments of inertia as a function of time, for parabolic initial orbits with different periastron distances. In order to exclude the noise introduced by the halo particles, we select from all particles those that have a local density lager than the median value and calculate the moments using only those particles. Initially the angular momentum is given in x-y plane in clockwise direction, that is the angular momentum vector points along the negative z-axis. In all runs the axis ratio is similar and is very stable in time.

Figure 8 shows the trajectory of the unit vector parallel to the major axis as a projection onto the x-y plane. In all models with non-zero initial angular momentum, the major axis of the resulting merger remnant is rotating in the same direction as the initial angular momentum. All models have clearly distinct major axe, and therefore they are not oblate. However, it is hard to see if they are triaxial or not and whether they are approaching a spherical/oblate structure or not.

Figure 9 shows the axis ratio as the function of the periastron distance of the initial orbit. For all runs, the axis ratio is averaged over the last three snapshots. It is somewhat counter-intuitive that figure 9 indicates that mergers are more prolate for collisions with larger angular momentum. However, with the relatively small number of particles we used, it is not yet clear whether this result is statistically significant.

Figure 10 shows the moments of inertia for collisions from a bound orbit. In this case, the merger remnant is clearly triaxial. Again, it is not clear whether the long-term evolution, including phase mixing, will lead to an oblate structure or not.

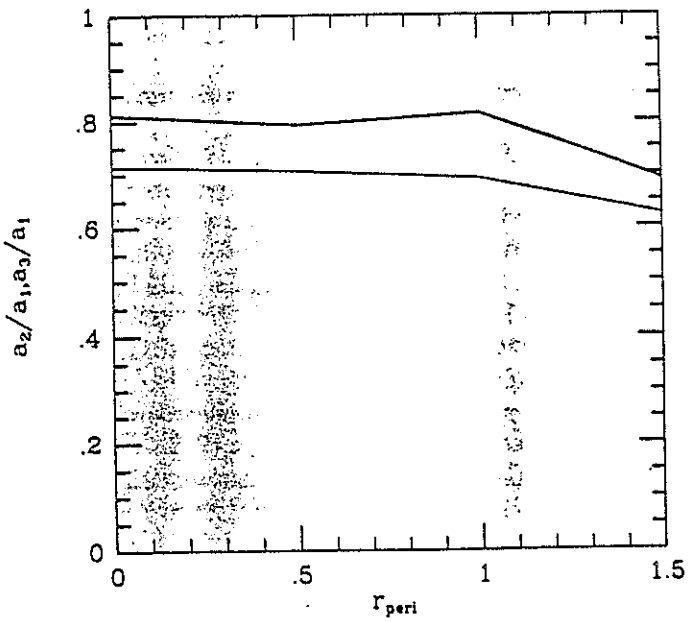

Figure 9: The axis ratios for the merger remnants of parabolic collisions as a function of r_{peri}. The upper full line indicates a_2/a_1, while lower dotted line indicates a_3/a_1.

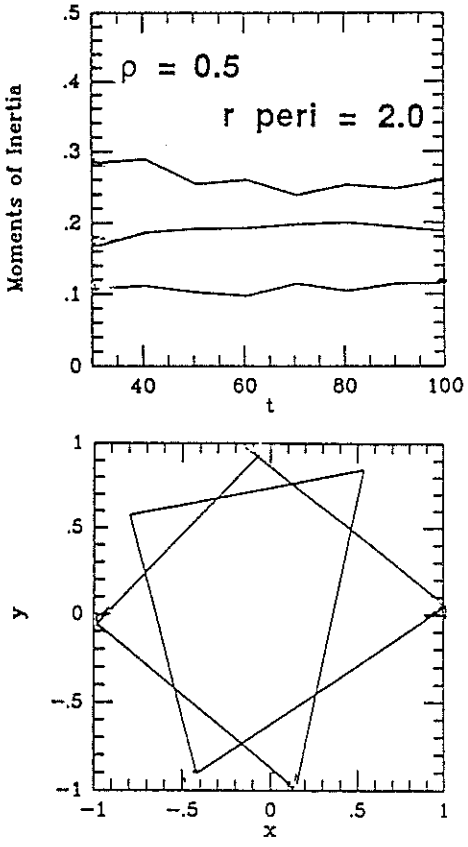

Figure 10: Same as figure 7 and 8 but for a collision from a bound orbit with eccentricity e=0.5 and r_{peri}=2. Note that the merger is clearly triaxial and rotating much faster than the mergers in figure 8.

Discussion

In this paper we have outlined the results of our experiments of collisions of two spherical galaxies. This is the first systematic survey performed by self-consistent N-body calculation with a number of particles large enough to obtain accurate results, while covering the wide range of collision parameters. We have measured the energy loss and mass loss as a function of collision parameters. For these quantities, the impulse approximation employed by Aguilar and White (1985) turned out to be reasonably good, although the impact approximation gives us no information about the structure of the galaxies after the collision.

Our N-body calculations suffer no such limitations, except for the particle noise and relaxation effects caused by the still small number of particles. For the global quantities such as the total mass or total energy, 2000 particles per galaxy gives very reliable results. However, this number is still too small to determine reliably the three-dimensional structure of the galaxies after the collision, as discussed earlier. It is clearly desirable to increase the number of particles to reduce the noise and relaxation effects. Current calculations take about 3 hours per run for the merging calculations. This duration is significantly longer than that for the non-merger case, because we need higher accuracy for a longer interval of real time. This calculation time happens to be quite similar for two completely different algorithms, namely the direct summation algorithm and the tree algorithm. The particle number 4000 is about the break-even point for these two algorithms. To decrease the particle noise and relaxation effects to 50% of the current values, we need to increase the number of particles by a factor of 4. For the direct summation this means that one run will require 50 hours, which is becoming excessive. For the tree algorithm one calculation would require ~15 hours, which is still large but feasible. For example, the John von Neumann Supercomputer Center will soon have an ETA10-G with 8 processors operating at a 7 ns clock cycle. Our algorithm is very easy to parallelize, both on coarse-grained machines and on fine-grained machines, and the efficiency is close to 100% (Makino 1988). Thus, one calculation could be performed 12 times faster than the current speed on one processor with a 10.5 ns clock cycle, which implies that one run will require only 75 minutes on the anticipated full version of the ETA10-G.

Acknowledgements

We would like to thank Joshua Barnes for useful discussions. The calculations were performed at the John von Neumann National Supercomputer Center, Princeton, NJ, USA.

References

Aarseth, S. J. 1985, in *Multiple Time Scales*, eds. Brackbill and Cohen (Academic Press), p. 377.

Aguilar, L. A. and White, S. D. M., 1985, *Astrophys. J.*, 295, 374.

Aguilar, L. A. and White, S. D. M., 1986, *Astrophys. J.*, 307, 97.

Appel, A., 1985, *SIAM J. Sci. Stat. Comput.* 6, 85.

Barnes, J., 1988, to appear in *Astrophys. J.*

Barnes, J. and Hut, P., 1986, *Nature*, 324, 446.

Heggie, D. C. and Mathieu, R. O., 1986, in *The Use of Supercomputers in Stellar Dynamics*, eds. S. McMillan and P. Hut (Springer), p. 233.

Hernquist, L., 1988, preprint.

Greengard, L. and Rokhlin, V., 1987, *J. Comp. Phys.*, 73, 325.

Jernigan, J. G., 1985, in *Dynamics of Star Clusters*, I.A.U. Symp. 113, ed. J. Goodman and P. Hut (Dordrecht: Reidel), p. 275.

Makino, J., 1988, preprint.

Miller, R. H., 1978, *Astrophys. J.*, 223, 1922.

Porter, D. 1985, Ph.D. thesis, Physics Department, University of California, Berkeley.

Press, W.H., 1986, in *The Use of Supercomputers in Stellar Dynamics*, eds. S. McMillan and P. Hut (Springer), p. 189.

Roos, N and Norman, C. A., , 1979. *Astron.Astrophys.*, 76, 75.

Toomre, A. and Toomre, J., 1972, *Astrophys. J.*, 178, 623.

van Albada, T. S. and van Gorkom, J. H., 1977, *Astron.Astrophys.*, 54, 121.

Villumsen, J. V., 1982, *Mon. Not. R. Astr. Soc.*, 199, 493.

Villumsen, J. V., 1983, *Mon. Not. R. Astr. Soc.*, 204, 219.

White, S. D. M., 1978, *Mon. Not. R. Astr. Soc.*, 184, 185.

White, S. D. M., 1979, *Mon. Not. R. Astr. Soc.*, 189, 831.

White, S. D. M., 1983, *Astrophys. J.*, 274, 53.

Appendix

Performance of our code on several supercomputers

Here we give results of the timing benchmarks of our code on several supercomputers. The machines we benchmarked are: ETA10-E (ETAVAST/FTN200), Cray X-MP/18 (CFT77), Cyber 205 (FTN 200), HITAC S-820/80 (FORT77/HAP V21-0A) and Facom VP-400 (FORTRAN77/VP V10L20). In table A-1 we give the CPU time per integration step for two different algorithms. One is the simple direct summation algorithm which we used for most of our calculations. The other is the hierarchical tree algorithm (Barnes and Hut 1986; for vectorization see Makino 1988 and Hernquist 1988). For both algorithms, we used the same Plummer model with the number of particles N=8192. For details of the benchmarks see Makino (1988). All calculations are performed using 64-bit words. On the ETA10 and the Cyber 205, calculation using 32-bit words is ~ 90% faster for the direct summation and ~25% faster for the tree algorithm. Note that all benchmarks are performed utilizing only one processor.

For the tree algorithm, the ETA10-E shows a significantly better performance than the Cray X-MP and a similar performance as the Facom VP-400. With our tree algorithm it is easy to take advantage of a multiprocessor system and the loss of efficiency is expected to be negligible. Therefore we predict that a ETA10-G with 8 processors running on a 7 ns clock cycle will run 12 times faster than the ETA10-E that we used, or more than 4 times faster than a Hitac S-820. Both the direct summation algorithm and the tree algorithm require relatively small amounts of memory ($50N$ words, where N is the number of particles and is $<10^5$). The amount of I/O we need is also quite small. Thus our calculation is completely CPU-bound, and the high peak performance of the ETA10 is ideal for our purpose.

Table A1: Performance of the Vectorized Code

Machine	Treecode (cpu sec/step)	Direct Summation (cpu sec/step)	Net Gain by Treecode
ETA10-E	1.75	8.42	4.8
CYBER 205	3.24	16.0	4.9
CRAY X-MP/18	2.83	11.6	4.1
Facom VP-400	1.79	2.93	1.6
Hitac S-8209/80	0.67	1.73	2.6